International Journal of Fluid Power 13 (2012) No. 1 pp. 41-50

COMPACT HELMHOLTZ RESONATORS FOR HYDRAULIC SYSTEMS

Nicholas E. Earnhart and Kenneth A. Cunefare

George W. Woodruff School of Mechanical Engineering, Georgia Institute of Technology,
771 Ferst Dr, Atlanta, GA 30332, USA
nick.earnhart@gatech.edu

Abstract

Noise is an ongoing concern in the fluid power industry. A great deal of research has been invested in reducing flow pulsations in hydraulic systems, from design modifications to adding noise control components. The physical principles of noise reduction are the same as for air, however, the much higher sound speed of hydraulic fluid makes creating compact noise control devices difficult. This paper introduces a Helmholtz resonator design that uses a compliant, voided urethane lining to increase the apparent volume of the device. The addition of the lining permits much smaller physical sizes for the same resonance frequency. Specifically, the design presented here has a total volume of 0.31 L and generates 20 dB of transmission loss at a resonance frequency of 37 Hz when the hydraulic system is pressurized at 2.07 MPa. At this pressure, it has a total volume that is two orders of magnitude smaller than a similar, unlined device of the same resonance frequency. Experimental data is presented that demonstrates the performance of the device. An analytical model was developed and least-squares fit to the experimental data to extract the complex bulk modulus of the liner material at hydrostatic pressures from 2.07 - 4.83 MPa, which is the range of available test pressures. This work is anticipated to lead to devices and liner materials designed for higher pressures.

Keywords: Helmholtz resonator, fluid-borne noise, compliant lining

1 Introduction

Helmholtz resonators are widely used as a convenient and effective way of reducing noise in a narrow band of frequencies. As such, they have been considered for use in fluid power systems for reducing the pressure ripple generated by positive displacement pumps. The design of Helmholtz resonators, in the simplest case, is governed by the sound speed in the resonator cavity and the geometric variables of neck length, neck area, and cavity volume. For devices in air, the speed of sound cannot be significantly modified; therefore design of these devices occurs through a give-and-take of the remaining geometric variables. The challenge for hydraulic systems is creating a device that is small enough for commercial use while being effective at frequencies low enough to match the fundamental frequency of the pressure source.

A number of authors have studied the use of Helmholtz resonators in hydraulic systems over the past two decades. Kojima and Edge (1994) and Lau, Johnston *et al.* (1994) studied the transmission loss of metallic-bellows style Helmholtz resonators. They reported resonance frequencies of 300 - 500 Hz, and the devices were quite small, with bellows gas volumes as low as 5.03 cm^3, with neck lengths from 23.0-48.2 mm. Kojima and Ichiyanagi (1998) and Kojima and Ichiyanagi (2000) studied the use of multi-volume side branches and Helmholtz resonators for the purpose of attenuating multiple frequency bands. Ijas and Virvalo (2000) also studied the use of an accumulator, side branches, and Helmholtz resonators. However, to achieve a resonance frequency of 50 Hz their Helmholtz resonator had a diameter of 8 cm and a neck that was 420 mm long; the authors acknowledged this was beyond practical limits for mobile machinery. Vael, López *et al.* (2004) designed a compact Helmholtz resonator with a resonance frequency of 3490 Hz to combat an internal resonance in their floating cup pump design. Kela (2008) and Kela and Vähäoja (2009) have also studied the use of Helmholtz resonators, specifically with the controllability of variable-volume devices.

Mikota and Manhartsgruber (2001) and Mikota and Reiter (2003) developed a type of compact, hybrid vibration absorber to be applied to hydraulic systems – essentially a tuned vibration absorber using a hydraulic volume as a spring. They reported transmission loss values of

This manuscript was received on 25 May 2011 and was accepted after revision for publication on 24 October 2011

15.2 dB at 225 Hz and 19 dB at 450 Hz for two variations of their design.

Bügener, Helduser *et al.* (2010) presented the use of a Helmholtz resonator for cavitation reduction. The zero-impedance boundary condition imposed by the entry of the resonator cancels the resonance frequency at the boundary. Therefore, by coupling the resonator close enough to the suction port, the negative-going pulses are less severe and cavitation effects may be abated. However, their device was both large (2L volume) and its resonance frequency did not appear to correlate with the fundamental pumping frequency of the system.

With regard to the use of linings with Helmholtz resonators, the only studies found in the literature have considered devices used in air systems. A Helmholtz resonator lined with a fibrous material was presented by Selamet, Xu *et al.* (2005) that demonstrated a frequency shift from the unlined case of up to 25 Hz. The frequency shift is attributed to the flow resistivity of the lining; increasing its thickness lowered the resonance frequency. An isothermal model for the sound propagation through the fibrous material could also account for a lower sound speed in the lining material, as found in Pierce (1989), thus making the resonator acoustically larger and shift the resonance frequency down. However, this phenomenon is not addressed by the authors.

For hydraulic oil, the speed of sound can be significantly modified from its nominal value of 1400 m/s by the use of a compliant lining. Previous work by Earnhart, Marek et al. (2010a) and Earnhart, Marek et al. (2010b) has demonstrated the effectiveness of such a lining in an in-line hydraulic silencer.

This work considers the use of a compliant lining in a Helmholtz resonator. Instead of being limited to geometric changes to modify the resonance frequency, the sound speed is changed through use of a compliant lining. This results in a device that is two orders of magnitude smaller than an unlined device of the same resonance frequency.

The Helmholtz resonators previously discussed in the literature are generally impractical for use in hydraulic systems, with the notable exception of the metallic-bellows style resonators studied by Kojima and Edge (1994) and Lau et al. (1994): either the resonator volume becomes very large or the length of the neck becomes impractically long. This work seeks to improve the compactness of noise control devices for fluid power - specifically, Helmholtz resonators. The size of the resonator is reduced by lowering the compliance of the resonator volume through the use of a voided urethane lining.

The fundamental theory of Helmholtz resonators will be discussed, followed by the formulation of a lumped-parameter model. The test rig used to measure the transmission loss of a prototype resonator will be presented, along with experimental data for the prototype resonator at varying static pressures. The output of the theoretical model will be compared against the appropriate experimental results, and the complex bulk modulus of the liner is given for system pressures in the range of 2.07 - 4.83 MPa. While these pressures are low for common industrial hydraulics, this is the pressure range of the available test equipment. This work is anticipated to lead to higher pressures and liner materials designed for such. Results will also be presented comparing a voided and unvoided liner in the prototype resonator to show the effect of the voiding on the performance of the resonator.

2 Modelling

The wavelengths of sound in hydraulic systems tend to be, at the frequencies considered, very long relative to the dimensions of a Helmholtz resonator. The fundamental frequency of a common 9-piston axial piston pump is 270 Hz; at this frequency the wavelength, λ, of sound in hydraulic fluid is over 5 meters assuming the speed of sound is c_0 = 1400 m/s. Therefore, a lumped parameter model works sufficiently well to model the behavior of the system, so long as any characteristic dimension of the device is much less than λ. The development of the model follows the derivation given in Kinsler, Frey et al. (1999). Fig. 1 is a schematic of a Helmholtz resonator with a compliant lining, and with resolved incident and transmitted waves and relevant dimensions. Fig. 2 indicates an analogous electric circuit model. The lumped parameter impedance of the resonator is given by

$$Z_{\mathrm{H}} = R + j\left(\omega L - \frac{1}{\omega C}\right) \tag{1}$$

where R, L, and C are the equivalent acoustic resistance, inductance, and compliance, respectively, and ω is the radian frequency. The resonance frequency occurs when the reactance ωL - 1 / ωC in Eq. 1 goes to zero. The compliance of the cavity is the inverse of the effective stiffness, which has contributions from the bulk modulus of both the fluid and liner. It is necessary, then, to find the compliance of the resonator considering the volume and bulk modulus of both media. Solving for the compliance, C, from Eq. 1 gives

$$C = \frac{1}{\omega_{\mathrm{r}}^2 L} \tag{2}$$

where ω_r is the resonance frequency and L is the inductance, given by

$$L = m / S_{\mathrm{n}}^2 \tag{3}$$

where m is the mass of fluid in the neck and S_n is the cross-sectional area of the neck. The mass m is a function of the density of the fluid and the cross-sectional area and length of the neck,

$$m = \rho_{\mathrm{f}} S_{\mathrm{n}} L_{\mathrm{n}}' \tag{4}$$

where the length of the neck is corrected to include acoustic radiation loading by

$$L_{\mathrm{n}}' = L_{\mathrm{n}} + 1.7 r_{\mathrm{n}}. \tag{5}$$

The bulk modulus is related to the speed of sound by

$$\beta = \rho c^2. \tag{6}$$

The effective stiffness of the resonator cavity is given in Kinsler et al. (1999), and is expressed as

$$s = \frac{\rho c^2 S_{\mathrm{n}}^2}{V}. \tag{7}$$

The compliance is the inverse of the stiffness, and substituting Eq. 6 into Eq. 7 for c^2 yields

$$C = \frac{S_{\mathrm{n}}^2}{s} = \frac{V}{\beta}. \tag{8}$$

For liner materials that exhibit viscoelastic behavior (the stress and strain are not in phase), the bulk modulus may be represented as a complex value, where the real part is the storage modulus and the imaginary part is the loss modulus as

$$\beta_{\mathrm{L}} = \beta_{\mathrm{L}}' + i\beta_{\mathrm{L}}''. \tag{9}$$

The ratio of the loss modulus to the storage modulus is referred to as the loss tangent or tan δ, and is a measure of the viscoelasticity of the material,

$$\tan\delta = \frac{\beta_{\mathrm{L}}''}{\beta_{\mathrm{L}}'}. \tag{10}$$

Thus, the liner introduces additional losses in addition to the acoustic radiation and viscous losses of the resonator (these latter losses are discussed below). If the resonator cavity has a compliant lining, the compliance of the cavity can be decomposed into the compliances of the liner and fluid acting in series, such that

$$C = C_{\mathrm{L}} + C_{\mathrm{f}} \tag{11}$$

where C_L represents the compliance of the liner and C_f represents the compliance of the fluid. Substituting Eq. 9 into Eq. 8 for the liner, and using Eq. 11 yields an equation for the compliance of the resonator cavity,

$$C = \frac{V_{\mathrm{L}}}{\beta_{\mathrm{L}}' + i\beta_{\mathrm{L}}''} + \frac{V_{\mathrm{f}}}{\beta_{\mathrm{f}}}. \tag{12}$$

Substituting Eq. (8) into Eq. (11) and rearranging gives

$$C = \frac{V}{\beta} = \frac{V_{\mathrm{L}}}{\beta_{\mathrm{L}}'} + \frac{V_{\mathrm{f}}}{\beta_{\mathrm{f}}} = \frac{V_{\mathrm{L}}\beta_{\mathrm{f}} + V_{\mathrm{f}}\beta_{\mathrm{L}}'}{\beta_{\mathrm{L}}'\beta_{\mathrm{f}}}. \tag{13}$$

Then, consider a liner that is much more compliant than the fluid, such that $\beta_{\mathrm{f}} >> \beta'_{\mathrm{L}}$, and has a similar volume $V_{\mathrm{L}} \sim V_{\mathrm{f}}$. Equation 13 becomes

$$C = \frac{V}{\beta} \simeq \frac{V_{\mathrm{L}}}{\beta_{\mathrm{L}}'} \tag{14}$$

which reveals that for a device with a liner that is much more compliant than the fluid, essentially all of the compliance of the cavity comes from the liner. Rearranging Eq. (2) yields an equation for the resonance frequency with respect to the compliance,

$$\omega_{\mathrm{r}} = \frac{1}{\sqrt{LC}}. \tag{15}$$

It can be easily seen from Eq. 15 that a larger value for the compliance of the cavity leads to a lower resonance frequency. From Eq. 12 raising the compliance requires either making the device larger or lowering the bulk modulus of the liner or fluid. Since the fluid has a fixed, high value of bulk modulus, introducing a liner that is significantly softer than the fluid is an effective way of raising the compliance, and thus lowering the resonance frequency for a given volume. Alternately, given a fixed resonance frequency, introduction of the liner lowers the required cavity volume.

The damping effects of the resonator need to be accounted for as well. First, the acoustic resistance of the fluid in the neck, including both viscous effects and radiation resistances, is

$$R = \left(R_{\mathrm{r}} + R_{\mathrm{w}}\right)/S_{\mathrm{n}}^2. \tag{16}$$

The radiation resistance is given from Kinsler et al. (1999) as

$$R_{\mathrm{r}} = \frac{\rho_{\mathrm{f}} c_{\mathrm{eff}} k_{\mathrm{eff}}^2 S_{\mathrm{n}}^2}{2\pi} \tag{17}$$

where $k_{eff} = \omega/c_{eff}$ is the effective wavenumber in the resonator, at the frequency considered. The effective sound speed in the resonator is given by

$$c_{\mathrm{eff}} = \sqrt{\frac{V}{\rho_{\mathrm{eff}} C}} \tag{18}$$

where the effective density is the total mass of the material in the cavity divided by its total volume. The derivation of the viscous resistance of the fluid motion in the neck begins with the approximation for the complex wavenumber for fluid lines given by Kojima and Edge (1994),

$$\xi = 1 + \sqrt{\frac{\upsilon}{j\omega r_{\mathrm{n}}^2}} + \frac{\upsilon}{j\omega r_{\mathrm{n}}^2}. \tag{19}$$

where υ is the kinematic viscosity of the fluid and r_n is the radius of the neck. The loss factor in the complex wave-number is determined by the ratio of the imaginary to complex part of the complex wave-number,

$$\alpha_{\mathrm{w}} = -\mathrm{Im}\left(k\xi\right)/\mathrm{Re}\left(k\xi\right). \tag{20}$$

Finally, the loss factor is used in the equation for the viscous resistance in the resonator neck, as given by Kinsler et al. (1999)

$$R_{\mathrm{w}} = 2m\omega\alpha_{\mathrm{w}}. \tag{21}$$

The transmission loss can be calculated from the elements of the transfer matrix for the resonator. The transfer matrix is

$$T = \begin{bmatrix} 1 & 0 \\ 1/Z_{\mathrm{H}} & 1 \end{bmatrix}. \tag{22}$$

The transmission loss is the input-output acoustic energy balance across a two-port device. The transmission loss of the resonator in a system with an infinite downsteam pipe (or anechoic termination downstream) can be calculated from the transfer matrix elements by

$$TL = 20\log_{10}\left[\frac{1}{2}\left|t_{11} + \frac{t_{12}}{Z_0} + Z_0 t_{21} + t_{22}\right|\right] \tag{23}$$

where t_{ij} are the transfer matrix elements and Z_0 is the characteristic impedance of the test pipe, given by

$$Z_0 = \frac{\rho_{\mathrm{f}} c_{\mathrm{f}}}{S} \tag{24}$$

where S is the cross-sectional area of the pipe.

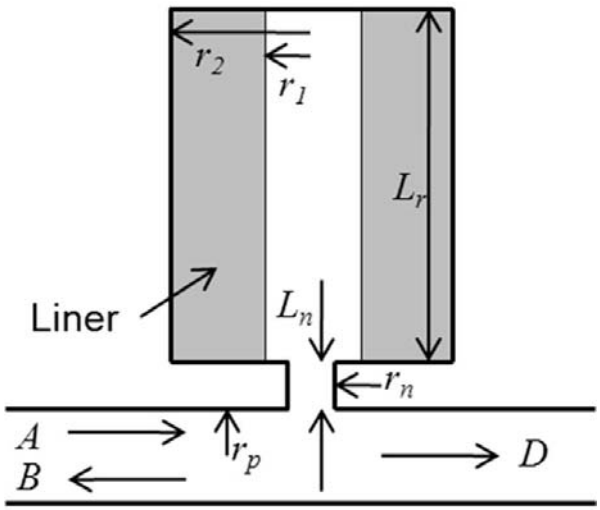

Fig. 1: *Helmholtz resonator with compliant lining*

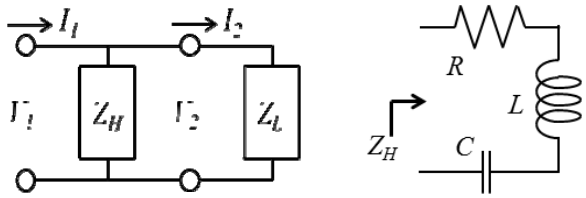

Fig. 2: *Helmholtz resonator electric circuit analogy*

A theoretical model for the transmission loss of a Helmholtz resonator has thus been developed. From a design perspective, it is of interest to evaluate the theoretical performance of the device given assumed material properties for the liner and fluid, and the impact of variation of the properties on the performance. First, consider two devices of identical neck geometry and resonance frequency. Then, Eq. 15 is used for comparison, such that

$$\frac{1}{L_1 C_1} = \frac{1}{L_2 C_2} \tag{25}$$

Since L is a function of the fluid density and neck geometry only, it is the same for both devices and $L_1 = L_2$ Substituting Eq. 8 for compliance C and rearranging yields

$$\frac{\beta_1}{\beta_2} = \frac{V_1}{V_2} \tag{26}$$

Therefore, the ratio of cavity volume between otherwise identical devices is directly proportional to the ratio of the effective bulk modulus of the material in the cavities. Assuming the introduction of the liner reduces the effective bulk modulus from that of the fluid alone, approximately 1.7 GPa, to 15.97 MPa, this leads to a volume reduction of a factor of 108. The device with the liner would be two orders of magnitude smaller than the unlined device, with all other aspects unchanged.

Likewise, the effect of introducing a liner to the cavity can be explored in terms of the transmission loss. Fig. 3 depicts the transmission loss of a Helmholtz resonator of the schematic in Fig. 1 and the dimensions in Table 1, for three configurations: no liner, a liner with a bulk modulus of 672 MPa, and a liner with a bulk modulus of 15.97 MPa. The resonance frequencies are 347 Hz, 228 Hz, and 37 Hz, respectively – since the resonance frequency is directly related to the effective bulk modulus of the cavity by

$$\omega_r = \sqrt{\frac{\beta}{LV}} \tag{27}$$

which is found from substituting Eq. 8 into Eq. 15. Through comparison of the lined vs. unlined *TL* predictions, it is evident that a significant reduction in the resonance frequency of two orders of magnitude may be obtained solely by introducing a compliant liner to the cavity. The peak *TL* decreases and quality factor increases as the resonance gets higher in frequency due to the viscous and radiation resistances, both which increase with increasing frequency.

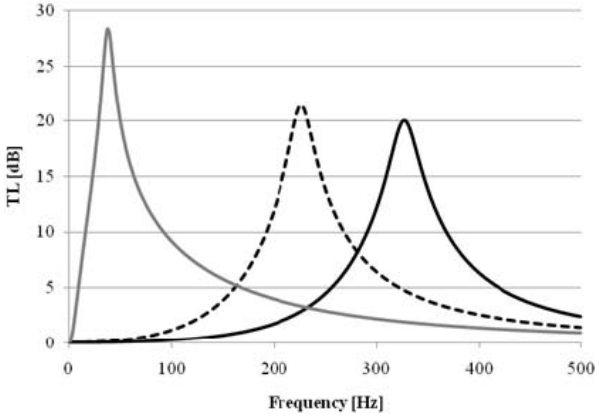

Fig. 3: *Theoretical model for Helmholtz resonator: ▬ No liner, ▪▪▪ Liner with β' = 672 MPa, ▬ Liner with β' = 15.97 MPa*

Table 1: Dimensions of Helmholtz resonator

	Inner Radius	Outer Radius	Length
Neck	-	2.97 mm	37.34 mm
Lining	13.30 mm	31.75 mm	97.28 mm

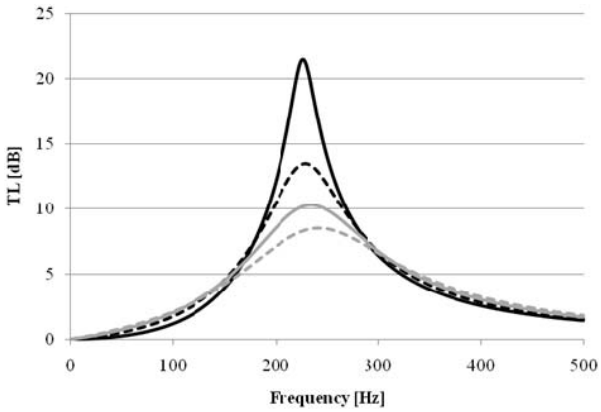

Fig. 4: *Theoretical model for lined Helmholtz resonator: ▬ Liner tan δ 0.0, 0.2, 0.4, 0.6▪▪▪*

The effect of increasing the losses in the liner by increasing the tan δ of the liner material can also be explored using the theoretical model. The transmission loss for a lined Helmholtz resonator, where the liner

has a bulk modulus of 672 MPa, is shown in Fig. 4 for liner tan δ values of 0.0 through 0.6. The implication of Fig. 4 is that the quality factor of the resonance, along with the maximum of the transmission loss, decreases with increasing tan δ, and can be modified independent of the resonator geometry through appropriate design or selection of the liner's material properties.

3 Experiment

3.1 Prototype

A prototype Helmholtz resonator was constructed per the schematic in Fig. 1, with its relevant dimensions indicated in

Table 1. The main chamber of the resonator is cylindrical with a cylindrical liner insert. There are two different liner materials of equivalent geometry for use with the resonator. The first is a voided urethane material, the second is an unvoided liner with properties similar to the host matrix of the voided liner.

3.2 Test Rig

A test rig was built to measure the transmission loss of two-port acoustic devices: a schematic of the rig is shown in Fig. 5. In order to determine the transmission loss of a two-port acoustic device, it is necessary to resolve both the forward- and reverse-travelling wave up- and downstream of the device. The two sections of pipe up- and downstream of the component under test are constructed according to the standard ISO-15086-2 (2000), since measurements in each section are used to determine the speed of sound. Of particular importance is the sensor spacing, which is 0.33 m between sensors 1 and 2 and 0.47 m between sensors 2 and 3 in each section, per the aforementioned standard. The sensors were calibrated to within 0.2 degrees relative phase at 40 Hz, and consistent data may be obtained as low as 10 Hz. A variable frequency drive controls a hydraulic power unit containing an axial-piston pump. A needle valve in the upstream line is left mostly open to generate broad-band noise in the flow. The mean flow is less than 10% of the speed of sound, so it is considered negligible. The termination silencer is a bladder-style, commercially-available hydraulic silencer and is mounted at the downstream end of the test section to isolate the test section from noise generated downstream. A needle valve at the downstream end serves as a load to regulate the static pressure at the component under test, measured by static pressure sensors. Six piezoelectric pressure transducers, three per side, are mounted flush with the inner surface of the rigid pipe and are unequally spaced to avoid a half-wavelength indeterminacy, as addressed by Johnston, et al. (1994). Data is acquired with a 24-bit data acquisition system mounted in a PC. The test method uses transfer functions to acquire and process data – the sensors were therefore calibrated relative to one another by mounting them circumferentially in a block, each exposed to the same acoustic pressure. To keep the noise floor low and improve the fidelity of the measurements, 100 vector averages are taken of the experimental transfer functions.

3.3 Test Method

The test method involves determining the acoustic pressure and velocity incident on the faces of the section of fluid exposed to the device under test. The up- and down-stream forward- and reverse-travelling waves are indicated in Fig. 3 as waves A, B, D, and E. To resolve the wave amplitudes, a least-squares regression is used to avoid half-wavelength indeterminacies that would otherwise occur between two sensors. The acoustic pressure in the upstream section of pipe can be expressed as

$$P = \left(Ae^{-\gamma x} + Be^{\gamma x} \right) e^{j\omega t} \tag{28}$$

where the acoustic velocity is given by

$$Q = \frac{Ae^{-\gamma x} - Be^{\gamma x}}{Z_0} e^{j\omega t} . \tag{29}$$

The downstream acoustic pressure and velocity are expressed in the same form as Eq. 28 and 29, interchanging D and E for A and B, and y for x, respectively. The impedance and wavenumber are given by

$$Z_0 = \frac{\rho c}{\pi r_p^2} \xi \ , \ \gamma = j \frac{\omega}{c} \xi \tag{30}$$

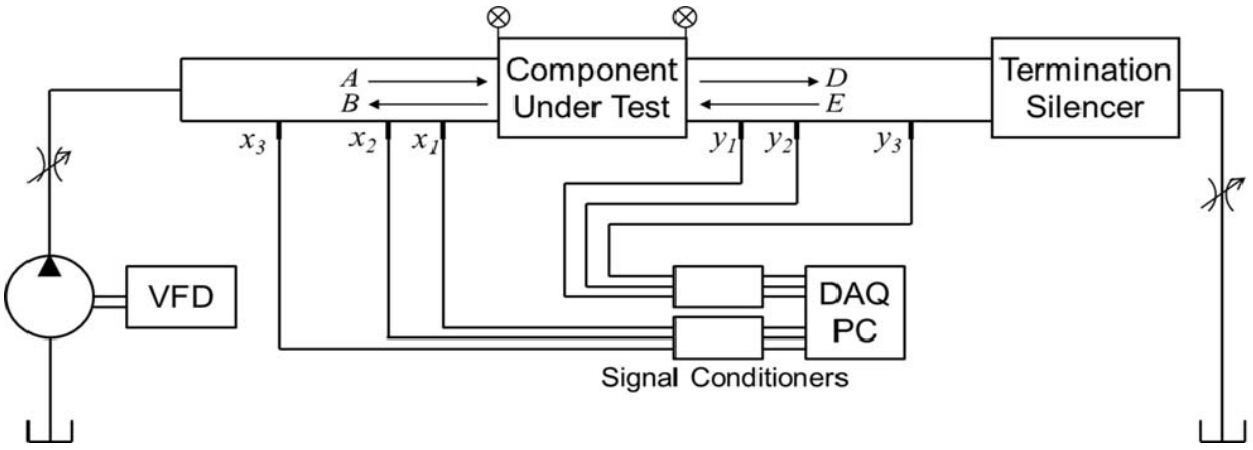

Fig. 5: *Schematic of test rig*

where an approximation to the viscous effects, given by Kojima and Edge (1994), is shown previously as Eq. 19. Here, r_p is the inner radius of the pipe and is used instead of r_n. The transfer matrix is given by

$$\begin{pmatrix} P_u \\ Q_u \end{pmatrix} = \begin{bmatrix} t_{11} & t_{12} \\ t_{21} & t_{22} \end{bmatrix} \begin{pmatrix} P_d \\ Q_d \end{pmatrix} \tag{31}$$

which is a set of two equations and four unknowns, where the subscripts *u* and *d* indicate the pressure at the upstream and downstream ports. This implies that two independent sets of experimental data are required to uniquely solve for t_{ij}. However, assuming that the transfer matrix section is symmetric and reciprocal, Pierce (1989) states that the determinant of the transfer matrix must be unity, which gives

$$t_{11}t_{22} - t_{12}t_{21} = 1 \tag{32}$$

and $t_{11} = t_{22}$, which reduces the number of unknowns to two. Using these assumptions and rearranging Eq. 31 yields a set of equations for the transfer matrix elements expressed in terms of the pressures and velocities calculated to be present at the upstream and downstream ports of the device in the system as tested:

$$\begin{aligned} t_{11} &= \frac{P_d Q_d + P_u Q_u}{P_u Q_d + P_d Q_u} \quad t_{12} = \frac{P_u^2 - P_d^2}{P_u Q_d + P_d Q_u} \\ t_{21} &= \frac{Q_u^2 - Q_d^2}{P_u Q_d + P_d Q_u} \quad t_{22} = \frac{P_d Q_d + P_u Q_u}{P_u Q_d + P_d Q_u} \end{aligned} \tag{33}$$

Of interest here is the device-specific transmission loss; that is, the transmission loss of the device that would be observed when installed in a system with an anechoic termination. Such is typically calculated by

$$TL = 20\log_{10}\left|\frac{A}{D}\right| \tag{34}$$

when an anechoic termination is realized. Since achieving an anechoic termination is difficult in practice, the transmission loss cannot be measured directly, rather, it must be calculated from the transfer matrix elements determined from the measured transfer functions between the sensors in the test rig. The transfer matrix method is able to determine the transfer matrix unique to the device regardless of termination, as was explored by Song and Bolton (2000) and which is evident in the papers of Kojima and Edge (1994), Johnston et al. (1994), and Lau et al. (1994). A key finding of the Song and Bolton paper is that one cannot simply use the resolved wavefields "*A*" and "*D*" to compute the *TL* that would be observed if the device was anechoically terminated unless the device actually was anechoically terminated when the transfer functions were measured. Physically, this is so because "*A*" and "*D*" are the wavefields that exist for the device as tested, for whatever the termination impedance may have been.

To explore this latter point in greater detail, note that through the definition of the elements of the transfer matrix elements, Eq. 33, it is possible to obtain an expression for the *TL* that would be observed with an anechoically-terminated device using the resolved wavefield observed when the device is not anechoically terminated. Since Eq. 33 include the total pressure and velocity at each face of the device, the respective terms are decomposed as

$$\begin{aligned} P_u &= A + B \quad P_d = D + E \\ Q_u &= \frac{A - B}{Z_0} \quad Q_d = \frac{D - E}{Z_0} \end{aligned} \tag{35}$$

Substituting the decomposed pressures and velocities in Eq. 35 into Eq. 33, then into Eq. 23 gives

$$TL = 20\log_{10}\left|\frac{A^2 - E^2}{AD - BE}\right| \tag{36}$$

Equation 36 accounts for the existence of a reverse-travelling wave in the downstream section. Due to the long acoustic wavelengths in hydraulic fluid, especially relative to the length of the pipe section immediately downstream of the device under test, this term cannot be ignored. However, if there existed an anechoic termination (or equivalently, an infinitely long downstream pipe) wave amplitude *E* would vanish and Eq. 36 would collapse to Eq. 34 which is the more familiar form of the transmission loss equation.

4 Results

The prototype Helmholtz resonator, with both the voided and unvoided urethane linings, was tested at static system pressures from 2.07 to 4.83 MPa in 0.34 MPa intervals (these pressures were a consequence of pressure limitations in the available test rig). The transfer matrix elements t_{ij} from Eq. 33 are shown in Fig. 7. The experimental transmission loss results for 2.07, 3.45, and 4.83 MPa are shown in Fig. 6. The resonance frequencies for each of the static pressures are approximately 37 Hz, 59 Hz, and 92 Hz, respectively. The maximum measured *TL* is 22.5 dB at 39 Hz at the 2.07 MPa pressure. The maximum *TL* decreases with increasing static pressure - this is a consequence of the pressure-stiffening behavior of the liner material.

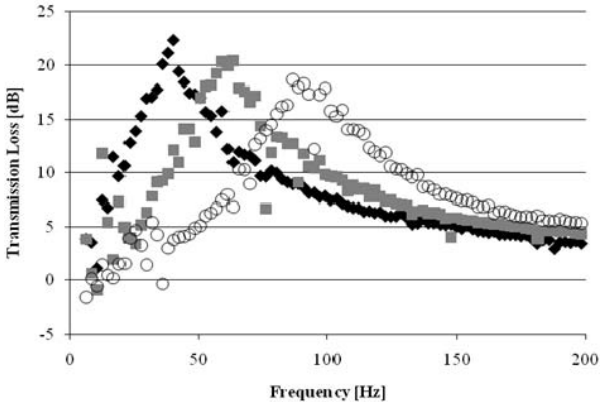

Fig. 6: *Transmission loss for prototype Helmholtz resonator: ♦ 2.07 MPa, ■ 3.45 MPa, ○ 4.83 MPa*

The analytical model was used within a least-squares routine to fit the model to the experimental data for the purpose of calculating the real and imaginary parts of the bulk modulus for the liner. The results of the least-squares fit for static pressures of 2.07, 3.45 and 4.83 MPa, using the voided liner, are given in Fig. 8 to 10. At each of the static pressures, the model underestimates the measured peak *TL* by 2 - 4 dB. At 2.07 MPa, the model overestimates the measured *TL* from 50 - 140 Hz

by approximately 1 dB. The least-squares fit appears to underestimate the damping in the liner; however, using a narrower band of frequencies to estimate the properties does not significantly change the results.

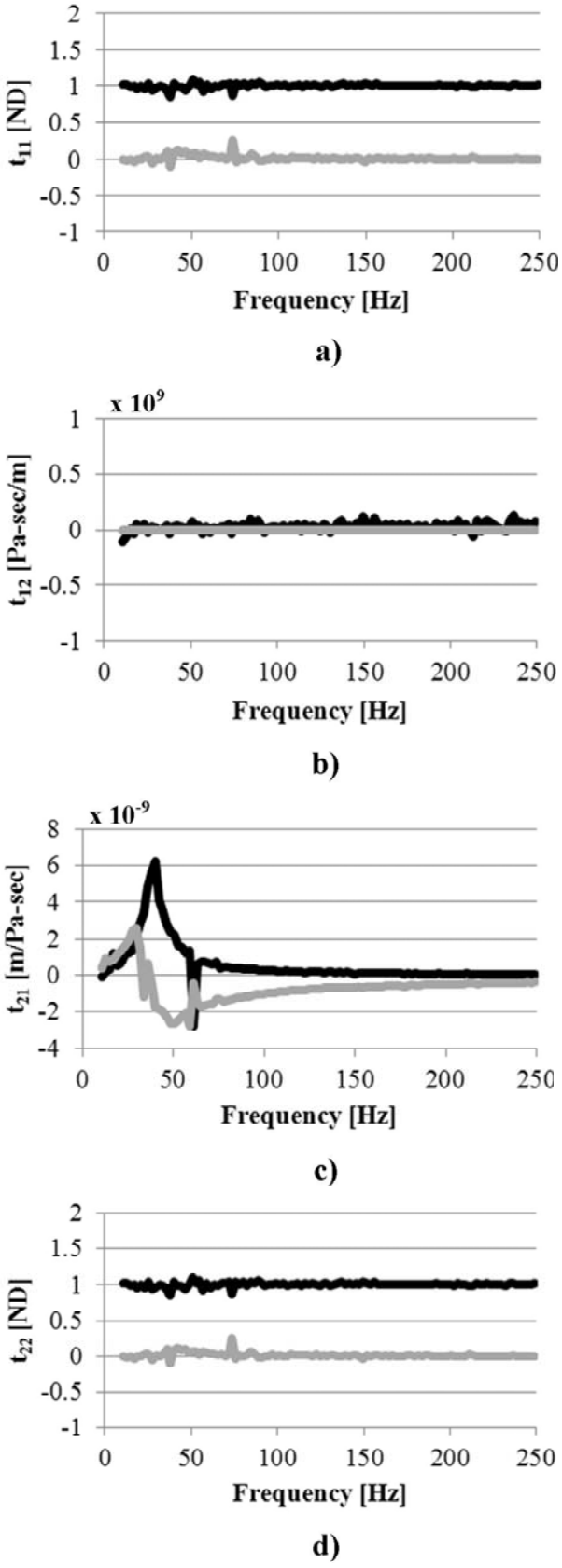

Fig. 7: *Transfer matrix elements for prototype Helmholtz resonator at 2.07 MPa. a) Term t_{11} b) Term t_{12} c) Term t_{21} d) Term t_{22}. For all plots, ▬ real part, ▬, imaginary part*

The resonance frequency for the Helmholtz resonator using both the voided and unvoided linings, as well as the calculated bulk modulus and tan δ are given in Table **2**. The tan δ is the loss in the liner only, separate from the losses due to radiation resistance and wall losses in the neck. The host materials of both liners have similar properties at atmospheric pressure; however, under hydrostatic pressure, the unvoided liner is much stiffer than the voided liner, and exhibits a much lower tan δ. The bulk modulus of the unvoided liner is 42 times higher at 2.07 MPa, and 14 times higher at 4.83 MPa.

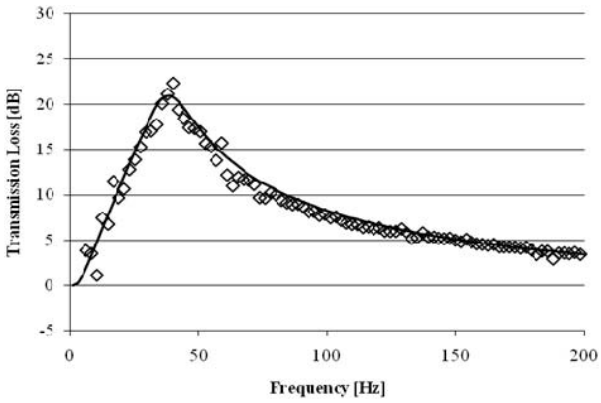

Fig. 8: *Transmission loss for prototype resonator at 2.07 MPa with lumped-parameter model: ◊ Experiment, ▬ Model*

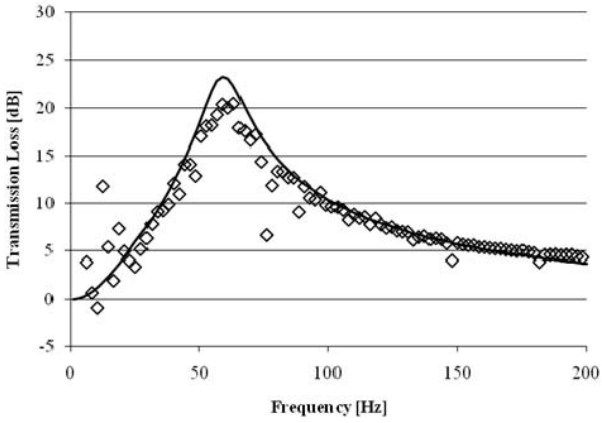

Fig. 9: *Transmission loss for prototype resonator at 3.45 MPa with lumped-parameter model: ◊ Experiment, ▬ Model*

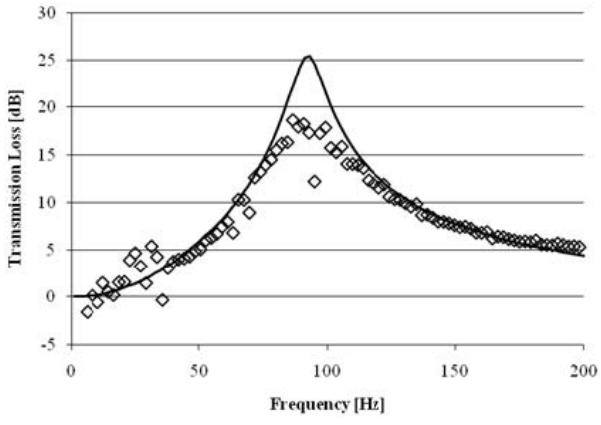

Fig. 10: *Transmission loss for prototype resonator at 4.83 MPa with lumped-parameter model: ◊ Experiment, ▬ Model*

Table 2: Resonance frequency for prototype Helmholtz resonator, with estimated bulk modulus for voided and unvoided urethane lining by static pressure

Static Pressure [MPa]	Voided lining			Unvoided lining		
	Resonance Frequency [Hz]	Bulk Modulus [MPa]	Tan Delta	Resonance Frequency [Hz]	Bulk Modulus [MPa]	Tan Delta
2.07	37	15.97	0.32	228	672.2	0.089
2.41	42	23.38	0.26	247	814.6	0.082
2.76	46	26.31	0.23	261	941.0	0.088
3.10	52	31.45	0.25	272	1040.2	0.081
3.45	59	39.56	0.24	283	1157.3	0.069
3.79	66	54.43	0.23	289	1215.5	0.071
4.14	74	63.93	0.17	295	1291.9	0.074
4.48	83	81.21	0.15	302	1381.5	0.052
4.83	92	99.71	0.17	308	1447.1	0.042

To put the size of the device and its resonance frequency in perspective, if the liner was not present in the resonator, it would have a resonance frequency of 347 Hz – an order of magnitude higher. Conversely, in order for an unlined resonator to have the same resonance frequency as the prototype at 2.07 MPa, the volume of the cavity would need to be 108 times larger than the lined device.

Figure 1 shows the transmission loss of the resonator with both the voided and unvoided liners at 2.07 MPa. The resonance frequency is higher for the unvoided liner, and is approximately 228 Hz. This indicates that the structure of the material is significant to the performance of the device under static pressure. The structure of the material is also controllable; thus, the resonance frequency may be varied independent of the size of the device through design and selection of the liner's material properties. This may lead to a device that can be tailored to attenuate different frequency bands simply by replacing the liner.

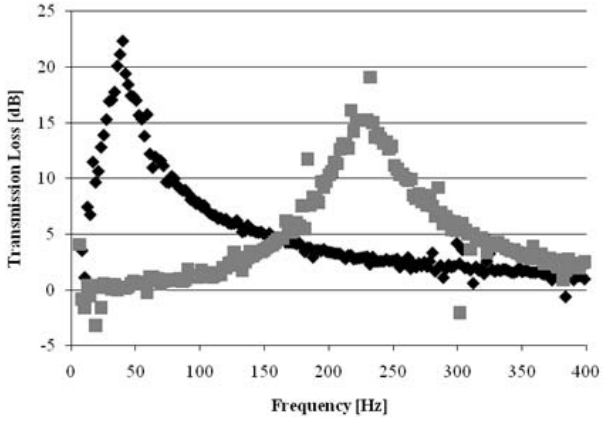

Fig. 11: *Prototype resonator at 2.07 MPa: ♦ Voided, ■ Unvoided*

5 Conclusions

A lumped-parameter model for a compact, prototype Helmholtz resonator for a hydraulic system has been presented, along with experimental data for the performance of the device. The model was used to calculate the bulk modulus of two compliant liners, one voided and one unvoided, using the experimental data. The prototype resonator exhibited resonance frequencies of 37, 59, and 92 Hz when used in a static pressure system of 2.07, 3.45, and 4.83 MPa, respectively. It has been demonstrated that the voiding of the urethane liner has a significant effect on the resonance frequency of the resonator when compared against an unvoided urethane lining. In addition, the volume of the prototype is 108 times smaller than that of an unlined resonator of equivalent neck geometry and resonance frequency when pressurized at 2.07 MPa.

Future work will involve varying the properties of the liner and the voiding. It is also of interest to test the device at higher pressures more common for hydraulic circuits, specifically, on the order of 20 MPa. A more sophisticated theoretical model is also in development to better understand and predict the impact of the liner.

Nomenclature

α_w	Loss factor	[ND]
β	Bulk modulus	[Pa]
β_f	Bulk modulus of fluid	[Pa]
β_L	Bulk modulus of liner	[Pa]
γ	Wavenumber	[1/m]
λ	Wavelength	[m]
ξ	Viscous effects	[ND]
ρ	Density	[kg/m^3]
ρ_{eff}	Effective density of cavity	[kg/m^3]
ρ_f	Density of fluid	[kg/m^3]
ρ_L	Density of liner	[kg/m^3]
ω	Radian frequency	[rad/sec]
ω_r	Resonance frequency	[rad/sec]
ν	Kinematic viscosity	[m^2/sec]
A,B,D,E	Wave amplitudes	[Pa]
c	Speed of sound	[m/s]
c_{eff}	Effective speed of sound	[m/s]
C	Equivalent capacitance	[m^2/kg]
C_f	Capacitance of fluid	[m^2/kg]
C_L	Capacitance of liner	[m^2/kg]
f	Frequency	[Hz]
j	$\sqrt{-1}$	[ND]
k	Wavenumber	[1/m]

k_{eff}	Effective wavenumber	[1/m]
L	Equivalent inductance	[kg/m^2]
L_n	Length of neck	[m]
L_r	Length of liner	[m]
P	Acoustic pressure	[Pa]
Q	Acoustic velocity	[m/s]
r_1	Inner radius of liner	[m]
r_2	Outer radius of liner	[m]
r_p	Radius of pipe	[m]
r_n	Radius of neck	[m]
R	Resistance	[kg/m^4-sec]
R_r	Radiation resistance	[kg/sec]
R_w	Viscous resistance	[kg/sec]
s	Equivalent stiffness	[N/m^3]
S	Area of test rig pipe	[m^2]
S_n	Area of resonator neck	[m^2]
t_{ij}	Transfer matrix element	[var]
T	Transfer matrix	-
TL	Transmission Loss	[dB]
V	Volume of resonator	[m^3]
V_f	Volume of fluid	[m^3]
V_L	Volume of liner	[m^3]
Z_0	Characteristic impedance	[Pa-sec/m^3]
Z_H	Impedance of Helmholtz resonator	[Pa-sec/m^3]
Z_L	Impedance of load circuit	[Pa-sec/m^3]

Acknowledgements

This research was supported by the Center for Compact and Efficient Fluid Power, a National Science Foundation Engineering Research Center funded under cooperative agreement number EEC-0540834. The authors are grateful for the support.

References

Bügener, N., **Helduser, S.** and **Weber, J.** 2010. Numerical analysis of a measure to improve the suction performance of hydrostatic pumps, *6th FPNI-PhD Symposium*. West Lafayette, IN.

Earnhart, N. E., **Marek, K. A.** and **Cunefare, K. A.** 2010a. Evaluation of hydraulic silencers, *NoiseCon10*. Baltimore, MD.

Earnhart, N. E., **Marek, K. A.** and **Cunefare, K. A.** 2010b. Modeling and Validation of an In-Line Hydraulic Silencer, *6th FPNI PhD Symposium*. West Lafayette, IN.

Ijas, M. and **Virvalo, T.** 2000. Experimental validation of pulsation dampers and their simplified theory, *Bath Workshop on Power Transmission and Motion Control*. University of Bath, UK.

ISO-15086-2. 2000. Hydraulic fluid power - Determination of fluid-borne noise characteristics of components and systems - Measurement of speed of sound in a fluid in a pipe. Geneva, Switzerland.

Johnston, D. N., **Longmore, D. K.** and **Drew, J. E.** 1994. A technique for the measurement of the transfer matrix characteristics of two-port hydraulic components. *Fluid Power Systems and Technology,* Vol. 1, pp. 25 - 33.

Kela, L. 2008. Resonant frequency of an adjustable Helmholtz resonator in a hydraulic system. *Archives of Applied Mechanics,* Vol. 79, pp. 11.

Kela, L. and **Vähäoja, P.** 2009. Control of an Adjustable Helmholtz Resonator in a Low-Pressure Hydraulic System. *International Journal of Fluid Power,* Vol. 10, pp. 10.

Kinsler, L. E., **Frey, A. R.**, **Coppens, A. B.** and **Sanders, J. V.** 1999. *Fundamentals of Acoustics*. 4th ed. John Wiley & Sons, Inc.

Kojima, E. and **Edge, K. A.** 1994. Experimental determination of hydraulic silencer transfer matrices and assessment of the method for use as a standard test procedure, *Innovations in Fluid Power, 7th Bath International Fluid Power Workshop*. University of Bath, UK.

Kojima, E. and **Ichiyanagi, T.** 1998. Development research of new types of multiple volume resonators, *Bath Workshop on Power Transmission and Motion Control*. University of Bath, UK.

Kojima, E. and **Ichiyanagi, T.** 2000. Research on pulsation attenuation characteristics of silencers in practical fluid power systems. *International Journal of Fluid Power,* Vol. 1, pp. 29-38.

Lau, K. K., **Johnston, D. N.** and **Edge, K. A.** 1994. Fluid borne noise characteristics of hydraulic filters and silencers, *Innovations in Fluid Power, 7th Bath International Fluid Power Workshop*. University of Bath, UK.

Mikota, J. and **Manhartsgruber, B.** 2001. Transient response dynamics of dynamic vibration absorbers for the attenuation of fluid-flow pulsations in hydraulic systems, *Bath Workshop on Power Transmission and Motion Control*. University of Bath, UK.

Mikota, J. and **Reiter, H.** 2003. Development of a compact and tuneable vibrations compensator for hydraulic systems. *International Journal of Fluid Power,* Vol. 4, pp. 17 - 30.

Pierce, A. D. 1989. *Acoustics: An Introduction to Its Physical Properties and Applications* Acoustical Society of America, Melville, NY.

Selamet, A., **Xu, M. B.**, **Lee, I.-J.** and **Huff, N. T.** 2005. Helmholtz resonator lined with absorbing material. *Journal of the Acoustical Society of America,* Vol. 117, pp. 725 - 733.

Song, B. H. and **Bolton, J. S.** 2000. A transfer-matrix approach for estimating the characteristic impedance and wave numbers of limp and rigid porous materials. *Journal of the Acoustical Society of America,* Vol. 107, pp. 1131 - 1152.

Vael, G. E. M., **López, I.** and **Achten, P. A. J.** 2004. Reducing flow pulsation with the floating cup pump - theoretical analysis, *Power Transmission and Motion Control*. University of Bath, UK.

Nicholas E. Earnhart
is a PhD candidate at the Georgia Institute of Technology. He obtained his BS in Mechanical Engineering from Purdue University in 2007, and his MSME at Georgia Tech in 2009. He has previously worked at GE and Rolls Royce.

Kenneth A. Cunefare
is a Professor at the Georgia Institute of Technology. He began at Georgia Tech in 1990. Prior he was the F.V. Hunt Postdoctoral Fellow at The Technical University of Berlin. He earned his PhD in 1990 from the Pennsylvania State University. He is currently Professor in Charge of the Integrated Acoustics Laboratory.